Electronic Supplementary Material

A. Optimal TL pulse for RISRS process

Before assessing chirp effects on a pulse's ability to generate ground state coherences, it's important to check its TL analogue. Using degenerate displaced harmonics model, invariance between pulse duration and vibrational frequency is expected. Our simulations show that a pulse duration of τ_0 which corresponds to the vibrational frequency (ν) as $\nu \cdot \tau_0 \cong 1/4$ is optimal for RISRS mechanism.

Fig. S1 shows the depth of modulation vs. the product of $\nu \cdot \tau_0$ for two modes: 1,600 cm^{-1} (solid blue) and 1,200 cm^{-1} (dashed red). As can be seen, the curves are not exactly similar, but the optimal pulse duration (given in terms of a fraction of the vibratioanl period) is very similar.

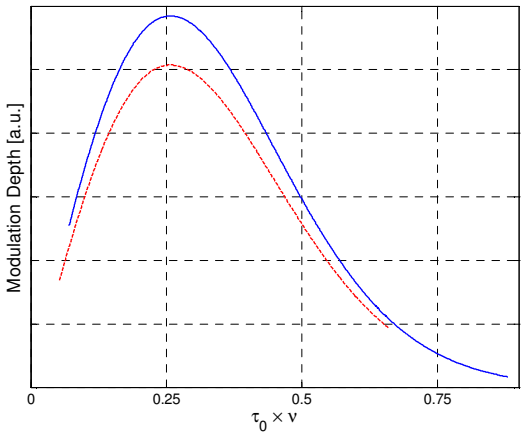

Fig. S1: Modulation depth vs. the product of TL pulse duration times the vibrational frequency ($\nu \cdot \tau_0$) for 1,600 cm^{-1} (solid blue) and 1,200 cm^{-1} (dashed red). TL pulse which corresponds to $\nu \cdot \tau_0 \cong 1/4$ is optimal for ground state modulations creation process.

This is similar to previous findings by Pollard et. al.[1], who suggested a value of 3/10 instead of a 1/4. It was rationalized as a duration which is long enough to allow wavepacket evolution on the excited state before dumping back to ground state, but not too long to prevent a creation of a delocalized "smeared" excited state wave packet.

B. Invariance and Displacement-Dependence

It's intriguing to check whether another invariance between pulse spectrum ($\propto 1/\tau_0$) and vibrational frequency (ν) exists also for the OC. Fig. S2 demonstrates that in the absence of dephasing, the optimal widening factor, namely $WF = \tau/\tau_0$, is invariant with respect to constant $\nu \cdot \tau_0$. The solid, dashed, dotted-dashed and dotted lines in the figure refer to $\Delta = 0.25, 1.00, 1.50, 2.00$, respectively. For a constant Δ, any pair $\{\nu, \tau_0\}$ is isomorphic with respect to w_F with any pair $\left\{\alpha\nu, \tau_0/\alpha\right\}$. Note that this statement is exact only with respect to w_F, but not with respect to ϕ'' or χ.

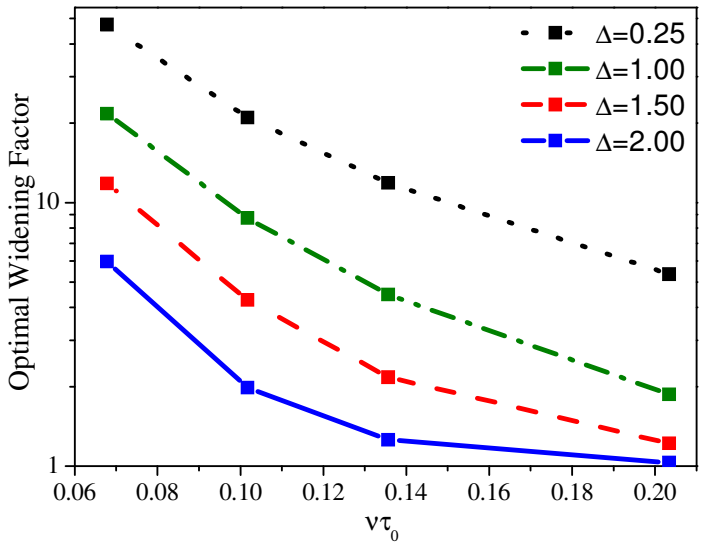

Fig. S2: Optimal widening factor (shown in a logarithmic scale) values vs. the invariant $\nu \cdot \tau_0$ (see text for details). The solid blue, dashed red, dotted-dashed green and dotted black lines represent $\Delta = 0.25$, 1.0, 1.5, and 2, respectively.

Moreover, for a constant $\nu \cdot \tau_0$, the larger the displacement – the smaller is the optimal widening factor, and correspondingly the smaller is the optimal chirp. This is also shown in Fig. 3 in the text and its following rationalization.

C. A Note on Non-Degenerate Oscillators

A first generalization of the theoretical section is the case where the ground state and excited state frequencies are non-degenerate, but still preserving the normal coordinates (neglecting Duschinsky's rotation).

Based on our rational regarding the scaling factor of ω^{-2} for the degenerate case, a similar reasoning leads here to suggest a scaling factor of $\omega_e\omega_g$ (the first corresponds to the "time window" of dynamic following and the latter to the vibrational quantum to be covered by the pulse).

Fig. S3 displays the modulation depth as a function of GVD for three cases, in which the product $\omega_e\omega_g$ is kept constant: the solid curve corresponds to degenerate oscillators with ω= 1600 cm^{-1}, the dashed line and the dashed dotted green line represent the modulation for ω_g = 1000, ω_e = 2560 cm^{-1}, and vice verse, respectively.

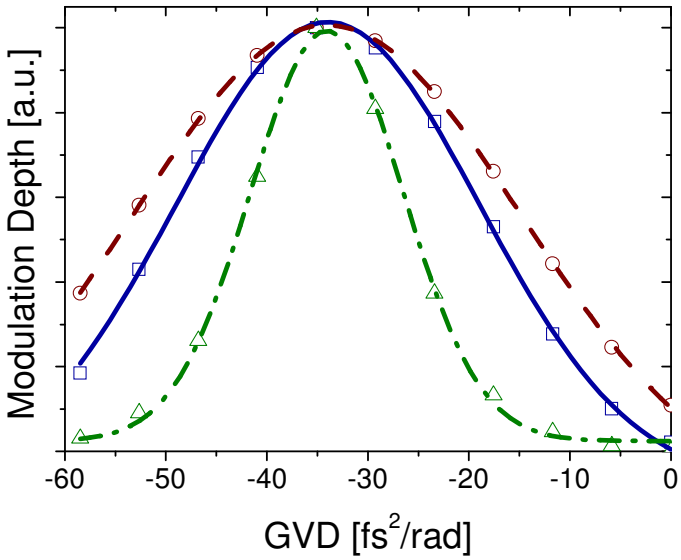

Fig. S3: The product rule: Modulation vs. GVD for non degenerate oscillators. The solid blue, dashed red, dotted-dashed green lines represent the results for $\omega_g = \omega_e$ = 1600 cm^{-1}, $\omega_g = 1000$ and $\omega_e = 2560$ cm^{-1}, and $\omega_g = 2560$ and $\omega_e = 1000$ cm^{-1}. The displacement is within small Δ regime. The rest of the parameters are $\tau_0 = 4.3$ fs, and $\delta = 0$. To account for zero point energy for the non-degenerate oscillators, the excited states are shifted by $\left(\omega_g - \omega_e\right)/2$.

The optimal chirp for all cases is similar, although the general behavior of the modulation for these parameters is different.

Fig. S4 shows the phases for the two paths in the non-degenerate cases, demonstrating that the absolute phases for each path are changes, but the optimal point (accounting for constructive interference) remains in tact. Moreover, to check the dependence of each path on ground and excited state frequencies, the cases of $\{\omega_g, \omega_e\} = \{1600, 1200\}$ and $\{1200, 1600\}$ cm^{-1} are displayed with circles and cross symbols, respectively. The results show that the roles of ground state and excited state are not symmetric. Whereas the phase of P_0 is insensitive to ω_e and depends only on ω_g (as expected), the phase of P_1 path is influenced by both.

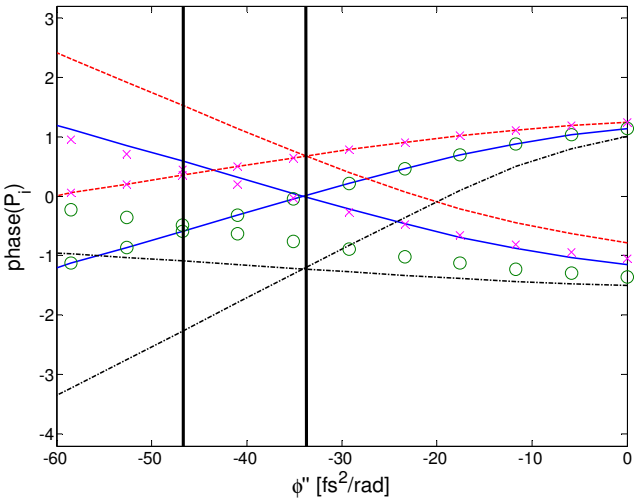

Fig. S4: Non-degenerate oscillators – phase analysis, same as Fig. 5 in the text. The solid, dashed and dotted-dashed lines refer to $\{\omega_g, \omega_e\} = \{1600, 1600\}$, $\{1200, 2133\}$ and $\{2133, 1200\}$ cm^{-1}, respectively. The circles and crosses refer to $\{\omega_g, \omega_e\} = \{1600, 1200\}$ and $\{1200, 1600\}$ cm^{-1}.

It is important to remark that this product rule is valid only for small displacements. Moreover, the simplicity of this interpretation directly leads us to suspect its validity for extreme ratios of ω_g / ω_e; for example, in the case of $\omega_g >> \omega_e$, where the build-up of the ground state non-stationary wavepacket is expected to be much slower than the excited state period. In this limit the product rule indeed fails.

D. Classical Estimate of Optimal Chirp in Large-Δ Regime

When Δ is large, a single vibrational quantum is small with respect to the coordinate dependence of the difference potential, allowing a classical estimate for OC. Assuming full impulsiveness of excitation a perfect reconstruction of the zeroth vibrational level of S_0 is generated on S_1. Upon its evolution, the overlap between the two nuclear wave functions for a single mode *j* will be:

$$(1)\ \langle \alpha_j \mid \alpha_j(t) \rangle = e^{-\frac{1}{2}|\Delta_j|^2(1-e^{-i\omega_j t})} \approx e^{-\frac{1}{2}|\Delta_j|^2(i\omega_j t+\omega_j^2 t^2/2+i\omega_j^3 t^3/6\ldots)}$$

When summing the contributions of the phase term from all modes and using short time approximation, we obtain:

$$(2)\ \Phi(t) = -\frac{1}{2}\left(\left(\sum_m |\Delta_m|^2\ \omega_m\right)\cdot t + \frac{1}{6}\left(\sum_m |\Delta_m|^2\ \omega_m^3\right)\cdot t^3\right)$$

We can assign a phase factor introduced to an effective field of mode j, caused by all modes other than j:

$$(3)\ \phi_j = \sum_{m\neq j}\frac{\Delta_m^2}{2}\left(\omega_m t - \omega_m^3 t^3 \Big/ 6\right)$$

The first term is irrelevant to the chirp (an arbitrary constant), but the latter – which must be compensated by the field if resonance is to be preserved – introduces a cubic chirp (TOD) to optimal field.

On the other hand, assuming that the electric field should follow the vertical difference potential for creation of an optimal ground state wavepacket[2], short time approximation for the place of the wave packet in the excited state yields a quadratic relation:

$$(4)\ \left\langle Q_e(t)\right\rangle = \Delta\cos\omega t \approx \frac{\Delta\omega^2}{2}t^2$$

Therefore, we conclude that a quadratic correlation exists between the difference potential and time:

$$(5)\ \Delta P_{ge}(t) = -\hbar\omega\Delta Q(t) = \frac{-\hbar\Delta^2\omega^3 t^2}{2}$$

Translating into frequency, we obtain: $\delta\omega(t) = \dfrac{\Delta P_{ge}(t)}{\hbar} = \dfrac{-\Delta^2\omega^3 t^2}{2}$.

The phase is obtained by integration over time: $\phi(t) = \int \delta\omega dt = \int \frac{\Delta^2 \omega^3 t^2}{2} dt = \frac{\Delta^2 \omega^3 t^3}{6}$.

As can be seen, we obtain a very similar relation to the one obtained before from calculation of the phase factor giving insight into chirp effects in the large-Δ regime, where the optimal chirp is indeed Δ-dependent (on the contrary to the low-Δ's scenario). This result shows clearly that in this regime chirp effects of different modes are correlated and not single mode characteristics.

E. PT Analysis – Detailed Discussion

In the discrete state representation, the wave function in either electronic state can be described as a superposition: $\left|\psi_{g/e}(x,t)\right\rangle = \sum_n c_n^{g/e}(t)\left|\phi_n^{g/e}(x)\right\rangle$

where $\left|\phi_n^{g/e}(x)\right\rangle$ are n$^{\text{th}}$ vibrational eigen-states of the ground/excited state potentials. The equations of motion for the coefficients are given by:

$$\begin{cases} \frac{dc_n^g}{dt} = n\hbar\omega_g c_n^g - \mu\varepsilon \sum_m F_{nm} c_m^e \\ \frac{dc_n^e}{dt} = \left(n\hbar\omega_e + \delta + \frac{\omega_g - \omega_e}{2}\right) c_n^e - \mu\varepsilon^* \sum_m F_{nm} c_m^{g*} \end{cases}$$

where $F_{nm} = \left\langle \phi_n^g \middle| \phi_m^e \right\rangle$ are Franck-Condon (FC) factors and $\frac{\omega_g - \omega_e}{2}$ accounts to the zero point energy shift. Expectation values for the position and momentum can be written:

$$\begin{cases} \left\langle x \right\rangle_{g/e} \propto \omega_{g/e}^{-1/2} \,\mathrm{Re}\left\{ \sum_n \sqrt{n+1} c_n^* c_{n+1} \right\} \\ \left\langle p \right\rangle_{g/e} \propto \mathrm{Im}\left\{ \sum_n \sqrt{n+1} c_n^* c_{n+1} \right\} \end{cases}$$

Thus, the modulation (M) is given by: $M \propto \sum_n \sqrt{n+1} c_n^* c_{n+1}$

Within the linear regime of excitation ("weak field"), the ground state coefficients fulfill $\left|c_0^g\right| \cong 1 \gg \left|c_{n\neq 0}^g\right|$, so that the sum in the expression for the modulation reduces to:

$$M_g \cong \left|c_0^g c_1^g\right| \cong \left|c_1^g\right|$$

Hence, in the absence of electronic dephasing, the modulation at the ground state is proportional to the population of the first vibrational excited state. In order to retrieve expressions for $c_n^{g/e}$ we use perturbation theory (PT), which is valid for fluences in the linear regime. Using first order PT, the amplitude of the excited state vibrational levels reads:

$$\left|n\right\rangle_e(t) = -\tfrac{i}{\hbar}\mu F_0^n \int_{-\infty}^{t} \varepsilon(t') \exp\left(-\tfrac{i}{\hbar}E_n^e(t-t')\right)\left|0\right\rangle_g dt'$$

where $E_n^e = n\hbar\omega_e + \delta + \frac{\omega_g - \omega_e}{2}$ is the energy of the n^{th} vibrational level within the excited electronic state manifold.

Explicit integration of the equation shows that the final excited state populations $\left|c_n^e\right|$ are chirp-independent. This is a manifestation of the well known Brumer-Shapiro theorem, which states that no control is attainable for operators that commute with the Hamiltonian and are influenced by single photon processes. Coherences of the ground state are second order in the field, and thus the Brumer-Shapiro theorem does not apply to them. Second order PT for $\left|1\right\rangle_g$ yields :

$$\left|1\right\rangle_g(t) = -\frac{i}{\hbar}\mu\sum_n F_1^n \int_{-\infty}^{t} \varepsilon^*(t')\left|n\right\rangle_e(t')\exp\left(-\tfrac{i}{\hbar}E_1^g(t-t')\right)dt' \equiv \sum_n \tilde{P}_n(t)$$

The generalization to multidimensional scenario is immediate. The wavefunction is written as a 2-D direct (tensor) product of the harmonic oscillators' basis set:

$$\left|\psi_{g/e}(x,y,t)\right\rangle = \sum_{n,m} c_{nm}^{g/e}(t)\left|\phi_{n_{g/e}}^x(x)\right\rangle \otimes \left|\phi_{m_{g/e}}^y(y)\right\rangle$$

The equations of motion for the expansion coefficients are similar to the one-dimensional one:

$$\begin{cases} \dfrac{dc_{nm}^g}{dt} = \hbar\left(n\omega_x + m\omega_y\right)c_{nm}^g - \mu\varepsilon\sum_{n',m'} F_{nm}^{n'm'} c_{n'm'}^e \\ \dfrac{dc_{nm}^e}{dt} = \hbar\left(n\omega_x + m\omega_y\right)c_{nm}^e - \mu\varepsilon^*\sum_{n',m'} F_{n'm'}^{nm} c_{n'm'}^{g*} \end{cases}$$

Where, as before, $F_{nm}^{n'm'} = \left\langle \phi_{n_g}^x \middle| \phi_{n'_e}^x \right\rangle \left\langle \phi_{m_g}^y \middle| \phi_{m'_e}^y \right\rangle$ are the FC factors.

The Feynman diagram for mode x within the interaction picture is shown in Fig. S5. Here also the amplitudes of different paths are determined by the FC factors. Looking at the diagram, we conclude that for the small displacements regime, the only paths that contribute to the modulation of the x(y) mode are P_{00} and P_{10}(P_{01}).

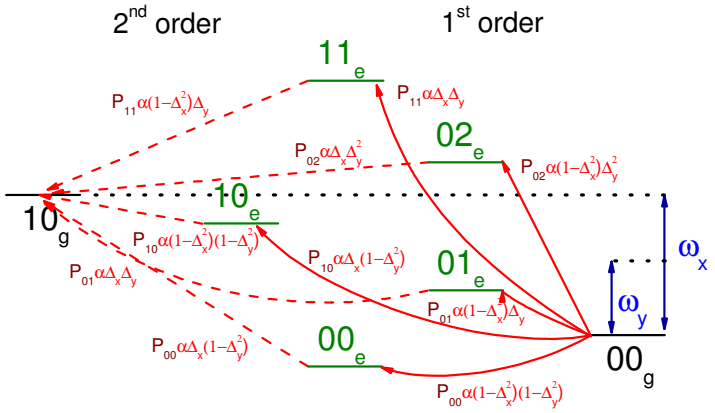

Fig. S5: Exemplar Feynman diagram for the modulation of the first mode. (right and left) First and second order coupling are denoted by arrows with the FC proportion denoted nearby.

F. PT for the Large Δ Regime

In the large−Δ regime, FC factors for more paths are substantial, leading to a more complex picture. Fig. S6 displays the absolute values and phases of the lowest four paths P_i, $i=0,1,2,3$, for $\Delta=1.03$ (upper panel) and $\Delta=2.06$ (lower panel).

Using second order PT, different paths don't interact with each other, so that the chirp-dependence phase of each path remains unchanged (see inset of the figure). The total modulation is changed mainly due to the addition of more paths, which have now significant FC factors. Moreover, higher paths correspond to off-resonance intermediate states, which absolute values fall off sharply with the GVD. These paths peak at the TL, therefore the optimal chirp shifts towards the TL as Δ is increased.

Semi-classically, the same trend is achieved when thinking of the wave-packets being far away from the minima of the excited state, where the slope of the potential curve is higher. This leads to faster dynamics, and therefore to lower optimal chirp.

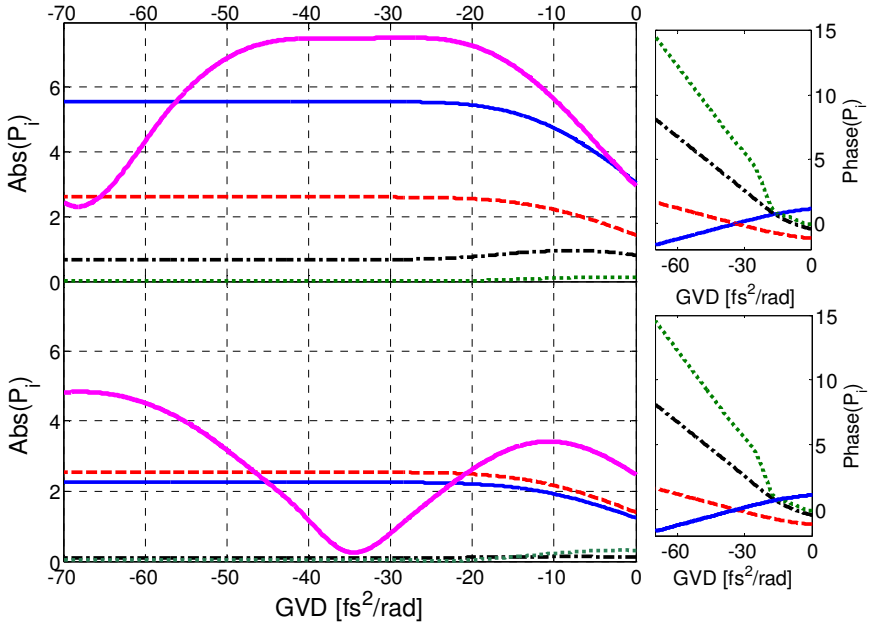

Fig. S6: Large displacement regime. (main) Absolute values of the path contributions. The solid, dashed, dotted-dashed, dotted, and extra thin lines refer to P_0, P_1, P_2 and P_3, respectively. The extra thick lines refer to the total modulation, or the sum of all of the paths. Upper and lower panels refer to displacement of Δ = 1.03 and 2.06. (inset) Phases of the paths.

G. Semi-quantitative approach to optimal chirp values

As shown in Fig. 5 in the text, within the small-displacements regime, the phase of the paths become linear-dependent on GVD for large chirps. As even the first optimal chirp point is within this linear regime, we'll denote:

$$\varphi_{0(1)} = \pm\frac{\pi}{2} + a_{0(1)}G$$

where $\varphi_{0(1)}$ is the phase of the $P_0(P_1)$ path, G is the GVD, and $a_0 = -a_1$.

The dependence of $a_0(-a_1)$ on the oscillator frequency for degenerate oscillators is plotted in Fig. S7, from which we conclude that $a_0 \propto \omega^2$. Therefore, we conclude that the optimal chirp: $G_{opt} \propto \omega^{-2}$, in accordance to simulation results and semi-classical reasoning described in text.

For non-degenrate oscillators, the product rule (stated earlier in the supplementary material, and shown in Fig. S4) applies. As can be seen, the dependence of each path on GVD changes due to the breaking of degeneracy; nonetheless, the phase-matching

(constructive interference) point remains the same, suggesting the validity of the product rule for this case.

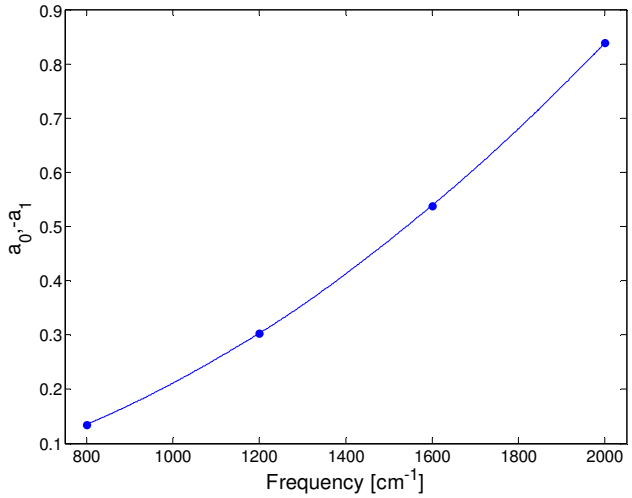

Fig. S7: Frequency dependence of the path's phase on the oscillator frequency.

Based on all these finding, and referring to cases where the product rule prevails, we "update" our formula for degenerate oscillators to be:

$$\varphi_0 = \frac{\pi}{2} - \frac{a}{\omega_g^2} G$$

$$\varphi_1 = -\frac{\pi}{2} + \frac{a}{\omega_g \omega_e} \left(2 - \frac{\omega_e}{\omega_g} \right) G$$

These formulae are valid also for the degenerate case, keeping also to the demand of $a_0 = -a_1$.

The first optimal chirp ($\varphi_0 = \varphi_1$) corresponds to:

$$G_{opt} = \frac{\pi \omega_g \omega_e}{2a}$$

The product rule for non-degenrate oscillators was achieved.

References

[1] W. T. Pollard, S. L. Dexheimer, Q. Wang, L. A. Peteanu, C. V. Shank and R. A. Mathies, *J. Phys. Chem.*, 1992, **96**(15), 6147-6158.
[2] E. R. Hiller and J. A. Cina, *J. Chem. Phys.*, 1996, **105**(9), 3419-3430.